Astron. Astrophys. 336, 1056–1064 (1998)

ASTRONOMY AND ASTROPHYSICS

A study of Hilda asteroids

III. Collision velocities and collision frequencies of Hilda asteroids

M. Dahlgren

Astronomiska observatoriet, Box 515, S-75120 Uppsala, Sweden

Received 28 August 1997 / Accepted 20 April 1998

Abstract. The collision velocities and collision frequencies of Hilda asteroids have been investigated numerically. The collision probabilities and collision velocities have been determined from a data base of close encounters, obtained by numerical integrations of the orbits of 909 asteroids for 55 000 years. The integration included all known main-belt, Cybele, Hilda, and Trojan objects larger than 50 km in diameter. The mean collision probability is lower for Hilda asteroids than for main-belt, Cybele and Trojan asteroids. Out of ten collisions involving a Hilda object, about seven are with main-belt objects, and the other three collisions are evenly distributed among the three outer-belt groups. The collision probabilities of individual Hilda asteroids have a strong correlation with the eccentricity of their orbits, resulting in a wide range (about a factor of six) of collision probabilities among the Hilda objects. The mean collision velocity of the Hilda asteroids is $4.6\,\mathrm{km\,s^{-1}}$, which is $0.5\,\mathrm{km\,s^{-1}}$ lower than the average for main-belt objects. The mean collision velocity of individual Hilda objects range from 3.3 to $6.0\,\mathrm{km\,s^{-1}}$.

Key words: asteroids

1. Introduction

Objects in the asteroid belt collide with each other due to the simple fact that they have elliptic orbits. Collisions of asteroids is believed to be an essential process behind the physical parameters of asteroids that we observe today, such as rotational properties, shapes, surface morphologies, and size distribution. Collision velocities and impact rates are also key factors to determine the lifetime of asteroids. In this paper, which is the third in a series about Hilda asteroids, their collisional properties will be investigated. See Dahlgren & Lagerkvist (1995), and Dahlgren et al. (1997) for the previous papers.

The first contributions to our understanding of collision velocities and impact rates in the main-belt have been made by Öpik (1951) and Wetherill (1967). Later studies by Farinella & Davis (1992) and Bottke et al. (1994) also used Wetherill's theory, which only needs the values of semi-major axes, eccentricities and inclinations of two objects to calculate the collision velocities and impact rate between them. Wetherill's theory was refined by Bottke et al. (1994) by also including the relative probability of all possible collision geometries between each asteroid pair, which earlier was assumed to be equal for all geometries. A different approach was taken by Vedder (1996) using a purely statistical method to derive the collisional properties of asteroids.

The collisional properties of the Trojan asteroids were studied by Marzari et al. (1996), performing numerical integrations of Trojan orbits, and analysing the close encounter data obtained during the numerical integration. They also included Hilda asteroids in their study because their orbits may intersect the orbits of Trojan asteroids.

The collisional properties of the Hilda asteroids have as yet not been studied as they were not included in the main-belt studies mentioned above. In the study by Marzari et al. (1996) main-belt objects were not included and therefore their results concerning the collision probabilities of the Hilda asteroids are of minor importance. Since the orbits of Hilda asteroids intersect orbits of both main-belt and Trojan asteroids, objects from the whole asteroid belt have to be accounted for to correctly investigate the collisional properties of Hilda asteroids. The aim of this paper is to determine the collisional properties of the Hilda population since these quantities are crucial when trying to improve our understanding of the rotational properties, shapes, and lifetimes of the Hilda asteroids. Extrapolating the collision probabilities and collision velocities from the main-belt studies or using the incomplete results from the Trojan study can lead to serious errors.

To study the collisional properties of the Hilda asteroids the equations of motion for a representative population of asteroids, from the inner parts of the main-belt to the Trojan clouds, have been numerically integrated and close encounters occurring between the asteroids have been detected. The close encounter data will be analysed to infer collision velocities and collision probabilities of objects in the asteroid belt. The analysis relies on the assumptions that there are no significant differences between the close encounter data and the objects that actually collide.

The advantage of the numerical method used in this study, compared to Wetherill's, is that the close encounter data will give accurate result even when the angular orbital elements of

Send offprint requests to: M. Dahlgren
Correspondence to: Mats.Dahlgren@astro.uu.se

the asteroids have non-random distributions or couplings between them. This is the case for Hilda and Trojan asteroids due to their residence in the 3:2 and 1:1 mean motion resonances with Jupiter. Ideally, the integrations should be carried out for a sufficiently long time span so that any temporary fluctuations in the osculating elements will be averaged out. In this study the numerical integrations were carried out for 55 000 years which is about equal to the longest period in the osculating elements of the Hilda asteroids. This is likely to average out any temporary fluctuations in the derived collisional properties due to the *ad hoc* starting time of the numerical integrations (see also Farinella & Davis 1992; Marzari et al. 1996).

In the analysis the asteroid population has been divided into four groups: main-belt, Cybele, Hilda and Trojan asteroids. The four groups gave ten 'collisional populations', namely: main-belt–main-belt (MM), Cybele–Cybele (CC), Hilda–Hilda (HH), L_4 Trojan–L_4 Trojan (TT_4), L_5 Trojan–L_5 Trojan (TT_5), Cybele–main-belt (CM), Hilda–Cybele (HC), Hilda–main-belt (HM), Hilda–L_4 Trojan (HT_4), and Hilda–L_5 Trojan (HT_5). These populations will be analysed separately, but the results will be discussed with emphasis on the Hilda asteroids since they are the primary concern of this paper. In the discussion of the collision velocities and collision probabilities the Trojan clouds have been treated as one unit, giving the Trojan–Trojan (TT) and the Hilda-Trojan (HT) collisional populations. Note that in the case of collision probabilities it has been taken into account that the Trojan clouds are two separate populations.

2. Asteroid sample and calculations

In an ideal case the asteroid sample should include all asteroids there is down to a relevant size limit. For instance, to obtain a complete picture of the collision properties of asteroids larger than 50 km in diameter, all asteroids larger than ~ 1 km (or even smaller) should be included in the sample. This ideal case is, however, for several reasons not obtainable. The number of asteroids larger then 1 km is not known, but is certainly to large to be handled easily computationally. To overcome this problem a representative sample of asteroids should be selected down to a size where the sample is reasonably complete and large enough that most types of orbits are represted in the sample. When these criteria are satisfied the collision probabilities and collision velocities determined should be close to the 'real' values obtained with a much larger population. This assumes that there are no significant differences between the orbits of the used population and the real population down to smaller sizes. Whether or not this is a valid assumption is difficult to assess, but it is a reasonable assumption to use.

In order to obtain a population as free as possible from observational biases, and representative of asteroids even in the outer-belt groups, all asteroids with $D \geq 50$ km were included in the asteroid sample. Most certainly, only a few asteroids with $D \geq 50$ km are still not discovered in the main-belt to Hilda region of the asteroid belt. (Cellino et al. 1991; Farinella & Davis 1992; Lagerkvist et al. 1996). In the Trojan region, however, there may be up to a factor of two more asteroids with $D \geq 50$ km than presently known (C.-I. Lagerkvist, private communication). The orbital elements are from Bowell (1997) and, when available, the asteroid diameters were taken from IRAS data (Tedesco & Veeder 1992). The diameters for asteroids with no IRAS diameter was estimated from the absolute magnitude H (Bowell et al. 1989) by assigning asteroids with a semi-major axis $a \leq 2.7$ AU an albedo $p_v = 0.15$, representative of S-type albedos, and when $a \geq 2.7$ AU, the albedos were set to $p_v = 0.04$ to mimic typical albedos of C-type surfaces. The change in p_v was made to approximate the compositional change with heliocentric distance seen in the asteroid belt. Tests showed that the obtained population is not sensitive to the exact value of p_v or the limit in semi-major axis. An asteroid sample of 909 asteroids was obtained (see Table 1 for details of their orbital properties).

Table 1. Orbital parameters for the asteroid sample. The number of objects N, range in semi-major axis a, mean and 1-σ of eccentricity e and inclination i are given for the four groups.

	N	a AU	⟨e⟩	⟨i⟩ deg
main-belt	680	2.20 - 3.26	0.14 ± 0.07	10.8 ± 6.1
Cybeles	46	3.33 - 3.77	0.10 ± 0.05	10.4 ± 6.4
Hildas	40[a]	3.87 - 4.01	0.16 ± 0.05	6.8 ± 4.1
Trojans	143[b]	5.08 - 5.33	0.08 ± 0.05	16.5 ± 8.3

[a] 273 Thule with a = 4.28 AU is included
[b] 76 are in the L_4 cloud and 67 in the L_5 cloud.

The equations of motion of the 909 asteroids were numerically integrated with the RADAU integrator (Everhart 1985) and with Jupiter and Saturn as perturbing planets. For each integration time step (set to 3 days) the distance between all asteroids (and planets) were computed. When the distance between two asteroids was less than 0.03 AU the position and velocity vectors for both asteroids were saved. However, for reasons explained below, only encounters with separation ≤ 0.02 AU were used in the analysis. The recorded close encounters have to be further processed to calculate the final values of the position and velocity vectors at the (true) minimum distance of each encounter. A more accurate minimum distance was searched for in the time interval $\pm$ 1.5 days, with a time step of 10 minutes with keplerian orbits of the two objects to obtain the final position and velocity vectors. The close encounter data will be biased towards low-velocity-deep encounters because the time spent by two asteroids within 0.03 AU from each other have an increasing probability to be less than the integration time step for high-velocity-shallow encounters. Therefore a significant part of these encounters will be lost. To get statistically unbiased close encounter data only encounters with distance ≤ 0.02 AU will be used in the analysis. Together with the time step of the numerical integration (3 days), this ensures that close encounters with relative velocities $\leq 26\,\mathrm{km\,s^{-1}}$ will be detected. This velocity is high enough to ensure that all close encounters occurring with the used asteroid sample will detected.

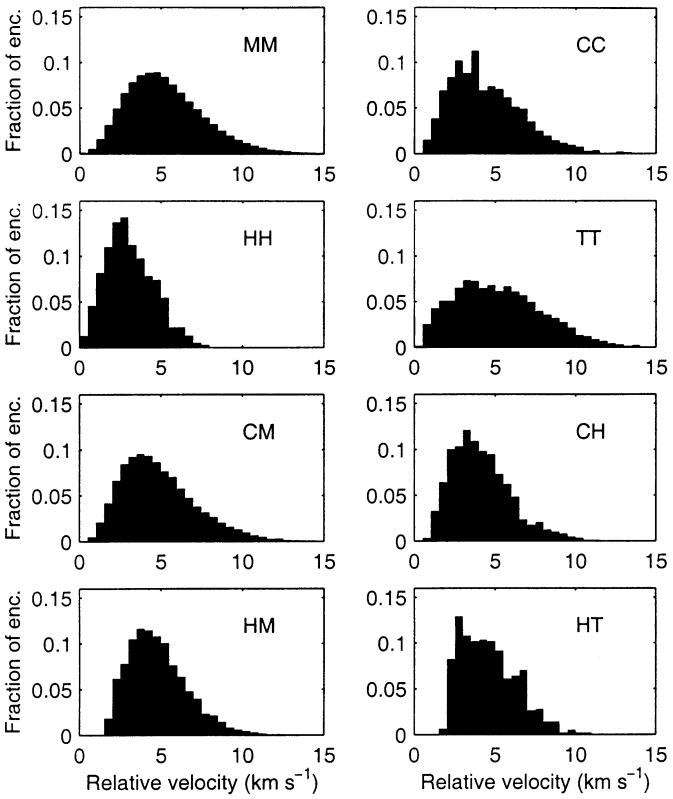

Fig. 1. Histograms of collision velocities for the different populations: **MM)** main-belt–main-belt, **CC)** Cybele–Cybele, **HH)** Hilda–Hilda, **TT)** Trojan–Trojan, **CM)** Cybele–main-belt, **HC)** Hilda–Cybele, **HM)** Hilda–main-belt, and **HT)** Hilda–Trojan collisions (see also Table 2). The bin size is $0.5\,\mathrm{km\,s^{-1}}$.

3. Collision velocities

From the obtained data base of close encounters, histograms of the collision velocities for the eight collision populations are shown in Fig. 1, and their mean, median and rms collision velocities are given in Table 2. Some general conclusions can be drawn from these histograms. There is a large spread in the collision velocities, from 1 to $15\,\mathrm{km\,s^{-1}}$. The high velocity tails and sharp cut-off at low velocities gives a clear non-Gaussian shape of the velocity distributions. There are also very narrow peaks in the velocity distributions probably from specific asteroid pairs making series of encounters at similar geometries (these are smoothed out by the binning in the histograms in Fig. 1). Considering the wide range in semi-major axes of the objects, the mean velocities are quite similar, ranging from 4.1 to $5.3\,\mathrm{km\,s^{-1}}$ in the different collisional populations, with one exception, HH collisions which have $\langle V\rangle$ = $3.1\,\mathrm{km\,s^{-1}}$. The velocity distribution of TT collisions have a less pronounced and broader peak than the other populations. The MM distribution have mean, median and rms velocities of 5.28, 4.97, and $5.78\,\mathrm{km\,s^{-1}}$, which is remarkably similar to the result by Bottke et al. (1994) in their Fig. 7, (5.29, 5.03, and $5.79\,\mathrm{km\,s^{-1}}$).

As mentioned above only mutual collisions among the Hilda asteroids have a significantly lower mean velocity. As pointed out by Marzari et al. (1996) there are three main reasons for this:

Table 2. The obtained mean, median, rms collision velocities, standard deviations, and number of close encounters for the populations and groups shown in Figs. 1 and 2.

Collisional population	$\langle V\rangle$ ($\mathrm{km\,s^{-1}}$)	V_{median} ($\mathrm{km\,s^{-1}}$)	V_{rms} ($\mathrm{km\,s^{-1}}$)	σ ($\mathrm{km\,s^{-1}}$)	N
MM	5.28	4.97	5.78	2.36	352715
CC	4.39	3.96	4.90	2.17	1372
HH	3.09	2.92	3.43	1.47	889
TT	5.20	4.93	5.84	2.67	14838
CM	4.89	4.53	5.38	2.26	22842
HC	4.12	3.87	4.50	1.81	1364
HM	4.78	4.55	5.10	1.78	8333
HT	4.59	4.35	4.90	1.71	663
Group					
main-belt	5.24	4.93	5.74	2.35	383890
Cybeles	4.82	4.46	5.31	2.24	25578
Hildas	4.56	4.33	4.91	1.82	11249
Trojans	5.17	4.89	5.80	2.64	15101

i) lower keplerian velocities at larger semi-major axes. ii) quite low eccentricities and inclinations of Hilda asteroids (Table 1). iii) a non-random distribution of the apsidal lines of the Hilda orbits preventing collisions between two Hilda asteroids if one is close to aphelion and the other is close to perihelion, which is the orbital configuration giving the largest relative velocity. The corresponding $\langle V\rangle$ for HH collisions in the study by Marzari et al. (1996) is $2.9\,\mathrm{km\,s^{-1}}$.

The mean collision velocity for HM is about $0.4\,\mathrm{km\,s^{-1}}$ lower than in MM collisions. This difference is quite small because the Hilda asteroids plunge into the outer parts of the main-belt when they approach their perihelia (i.e., at their highest orbital velocity), and will collide with main-belt objects having higher keplerian velocities. The mean velocity of HC collisions is about $1.1\,\mathrm{km\,s^{-1}}$ lower than MM collisions, mainly due to lower keplerian velocities of the objects in the Cybele and Hilda groups.

The mean collision velocity of Trojan asteroids are similar to the main-belt value, despite the lower keplerian velocities at the heliocentric distance of the Trojan clouds. This is fully compensated by a higher mean inclination of the Trojan asteroids compared to main-belt objects (Table 1). The collision velocities of the Trojan asteroids is likely to increase when the Trojan sample is complete, due to the discovery bias against high inclination Trojan asteroids. This bias arises from from the observing strategy applied by most surveys (i.e., they only search for objects relatively close to the ecliptic plane). This is consistent with our result, which is about $0.2\,\mathrm{km\,s^{-1}}$ higher than the result by Marzari et al. (1996) which used a smaller sample (114 Trojans) which had a smaller mean inclination ($\langle i\rangle = 15.5°$) compared to the sample used in this paper $\langle i\rangle = 16.5°$. The collision velocity distributions of the four groups (Fig. 2 and Table 2) are similar to the dominating collision population in each group, (i.e., MM, CM, HM, and TT collisions for main-belt, Cybele, Hilda, and Trojan asteroids, respectively).

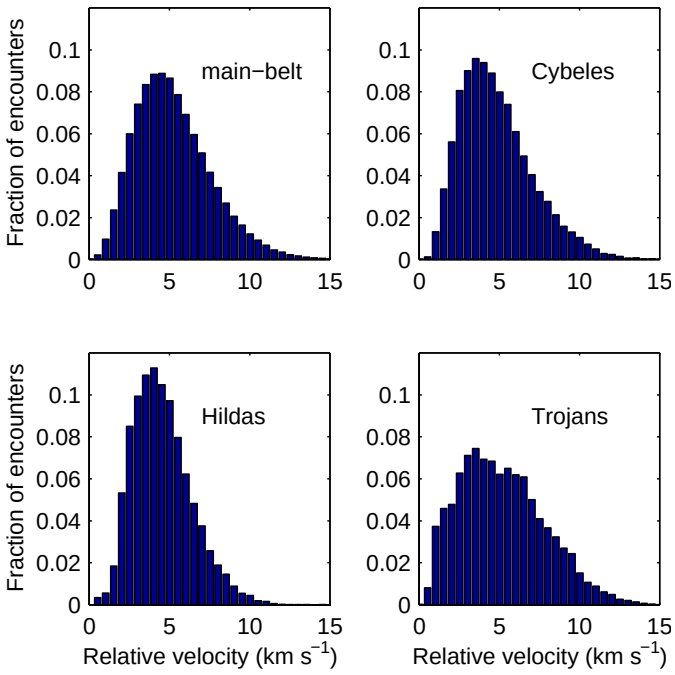

Fig. 2. Histograms of the obtained collision velocities for main-belt, Cybele, Hilda and Trojan asteroids. The bin size is 0.5 $\mathrm{km\,s^{-1}}$.

Table 3. The obtained collision velocity components $V_\mathrm{x}, V_\mathrm{y}$, and V_z of the populations. The mean and standard deviations of the relative velocity components are given.

	$\langle \mid \mathrm{V_x} \mid \rangle$ ($\mathrm{km\,s^{-1}}$)	$\langle \mid \mathrm{V_y} \mid \rangle$ ($\mathrm{km\,s^{-1}}$)	$\langle \mid \mathrm{V_z} \mid \rangle$ ($\mathrm{km\,s^{-1}}$)	$\sigma_{\mathrm{V_x}}$ ($\mathrm{km\,s^{-1}}$)	$\sigma_{\mathrm{V_y}}$ ($\mathrm{km\,s^{-1}}$)	$\sigma_{\mathrm{V_z}}$ ($\mathrm{km\,s^{-1}}$)
MM	1.87	1.87	3.86	1.42	1.42	4.65
CC	1.08	1.10	3.78	1.41	1.43	4.46
HH	1.21	1.22	1.97	1.69	1.74	2.42
TT	0.86	0.76	4.97	1.10	0.98	5.65
CM	1.57	1.55	3.83	1.98	1.97	4.60
HC	1.67	1.64	2.81	2.01	1.99	3.47
HM	2.08	2.12	3.04	2.46	2.38	3.71
HT	1.41	1.46	3.70	1.55	1.64	4.27

3.1. Velocity components of the collisions

The Cartesian velocity components ($V_\mathrm{x}, V_\mathrm{y}, V_\mathrm{z}$) of the collisions are given in Table 3, which lists the mean velocities and the standard deviations for the populations. The $\langle V_\mathrm{z} \rangle$ components (i.e., perpendicular to the ecliptic plane) are 1.5–5.0 times larger than the corresponding $\langle V_\mathrm{x} \rangle$ and $\langle V_\mathrm{y} \rangle$ components. The populations involving Hilda asteroids (HH, HM, HC, and HT) have $\langle V_\mathrm{z} \rangle$ / $\langle V_\mathrm{x} \rangle$ in the lower part of this range, from $\langle V_\mathrm{z} \rangle$ / $\langle V_\mathrm{x} \rangle$ = 1.5 for HH collisions to $\langle V_\mathrm{z} \rangle$ / $\langle V_\mathrm{x} \rangle$ = 2.2 for HT collisions. This is due to the low mean inclinations of Hilda asteroids ($\langle i \rangle$ = 7°) giving a more isotropic distribution of the velocity components than in the other groups. This leads to the conclusion that the inclinations of the orbits to a large extent determine the relative velocities in the asteroid belt, which is consistent with the result from earlier investigation (Farinella & Davis 1992; Bottke et al. 1994; Marzari et al. 1996).

4. Collision probabilities

With the number of close encounters recorded for each population (given in Table 2), we can obtain a first glimpse of the relative importance of the different populations to the total collision probability of the Hilda asteroids. Collisions experienced by Hilda asteroids are dominated by HM collisions (74%), whereas the low velocity HH collisions only contribute 7% to the number of collisions involving Hilda asteroids. Similar contributions come from the HC and HT collisions, which add respectively, 10% and 7% to the number of collisions involving Hilda objects. The results for the other groups show that the Trojan asteroids collide with themselves (in their respective two clouds) and to a small extent (5%) with Hilda asteroids. Collisions involving objects from the Cybele group are mostly from the MC collisions (91%) with small contributions from CC (5%) and HC (4%) populations. Collisions involving main-belt objects have small contributions from the CH (5%) and the HM (2%) populations added to their total number of collisions.

4.1. Intrinsic collision probability

To obtain more quantitative results the close encounter data have been used to calculate the intrinsic collision probability P_i between objects (Wetherill 1967). The intrinsic collision probability describes the probability for collision between two objects, and P_i is the probability of collision between two objects with $r_1 + r_2$ = 1 km, where r_1 and r_2 are their respective radii. The intrinsic collision probability is only dependent on the orbital elements of the two objects, and when two orbits do not intersect the intrinsic collision probability is zero.

The number of close encounters N within a specific distance R to an object is expected to be a function of the form $N \propto R^2$, because the cross section of a close encounter is πR^2. To verify this the number of close encounters as a function of distance were calculated for some of the asteroids, and the best fitting $N \propto R^2$ function were determined. The results for three Hilda asteroids are given in Fig. 3. The encounter data of these Hilda objects were selected to validate that the $N \propto R^2$ approximation is acceptable for wide ranges in N, orbital eccentricity and inclination of the objects.

Using the $N \propto R^2$ dependence, where N is the number of close encounters within a specific distance (in this case R = 0.02 AU), the intrinsic collision probability of an object is

$$P_\mathrm{i} = \frac{N}{n_\mathrm{p} T R^2} \qquad (1)$$

where T is the time interval used to obtain N close encounters, and n_p is the number of possible collision pairs in the interaction population(s). In the case of the MM, CC, HH, $\mathrm{TT_4}$, and $\mathrm{TT_5}$ populations, each object is a possible target for all the other $n-1$ objects in the population, giving $n_\mathrm{p} = n(n-1)/2$ possible pairs. In the case of the other collisional populations (CM,

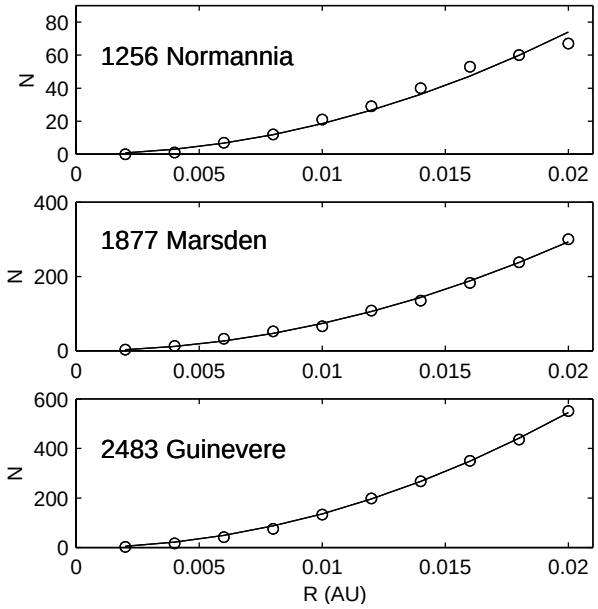

Fig. 3. Number of encounter as a function of distance for three Hilda asteroids and the best fitting $N \propto R^2$ functions.

HM, HC, and HT) the number of possible pairs is $n_{\rm p} = n_1 n_2$ where n_1 and n_2 are the number of objects in the respective population. When calculating the $P_{\rm i}$ for objects with respect to all interacting populations the number of pairs were calculated as $n_{\rm p} = n_{\rm int} + n_{\rm ext}$ where $n_{\rm int} = n_1(n_1 - 1)/2$ is the number of internal pairs and $n_{\rm ext} = \sum_{i=2}^{k} n_1 n_{\rm i}$ is the number of external pairs between the $k - 1$ interacting populations. Since $P_{\rm i}$ is the collision probability per cross section unit ($\rm km^{-2}$) of the object, the total collision probability of an object can be obtained by multiplying with the actual cross section of the object in question.

The intrinsic collision probability of each object has been calculated with Eq. 1, and the resulting mean intrinsic collision probability $\langle P_{\rm i} \rangle$ of the different populations are given in Table 4, where the given dispersions are the standard error of the mean. Also the calculated $\langle P_{\rm i} \rangle$ for the main-belt, Cybele, Hilda, and Trojan groups are given in Table 4.

Among the collisional populations involving Hilda asteroids, the highest $\langle P_{\rm i} \rangle$ was found for HH collisions. However, the small Hilda population results in a small contribution to the total collision probability of Hilda asteroids. The determined $\langle P_{\rm i} \rangle$ of HH collisions is 14% lower than the value obtained by Marzari et al. (1996). This difference can be due to the different (larger) Hilda population which has slightly different orbital parameters used by Marzari and co-workers. However, a more plausible explanation comes from the fact that their numerical integrations were carried out for about $1.1\times\ 10^4$ years, thereby not allowing the longest period in the osculating orbital eccentricity of the Hilda orbits to complete a whole cycle. This can give a biased $\langle P_{\rm i} \rangle$ since the collision probability of the Hilda objects varies with time as the shape of their orbits varies with time (around a stable mean value).

Table 4. Mean intrinsic collision probability $\langle P_{\rm i} \rangle$ for the collisional populations and for the main-belt, Cybele, Hilda, and Trojan groups.

	$\langle P_{\rm i} \rangle$ $10^{-18}\,\rm km^{-2}\,yr^{-1}$
MM	3.10 ± 0.02
CC	2.69 ± 0.10
HH	2.31 ± 0.10
TT	5.94 ± 0.10
CM	1.48 ± 0.07
HC	1.51 ± 0.06
HM	0.62 ± 0.04
HT	0.24 ± 0.06
main-belt	2.87 ± 0.03
Cybeles	1.53 ± 0.01
Hildas	0.68 ± 0.03
Trojans	3.86 ± 0.10

Table 5. Mean collision probability $\langle P_{\rm H} \rangle$ for the collisional populations involving Hilda asteroids, and for the main-belt, Cybele, Hilda, and Trojan groups.

	$\langle P_{\rm H} \rangle$ $10^{-18}\,\rm km^{-2}\,yr^{-1}$
HH	1.13 ± 0.05
HC	1.82 ± 0.08
HM	11.1 ± 0.67
HT	0.89 ± 0.12
main-belt	56.4 ± 0.41
Cybeles	27.6 ± 1.13
Hildas	16.0 ± 0.83
Trojans	11.0 ± 0.34

The $\langle P_{\rm i} \rangle$ for HM collisions are much lower than for HH collisions, this is mainly due to that HM collisions only are possible when Hilda asteroids are close to their perihelia. An even lower $\langle P_{\rm i} \rangle$ was found for HT collisions, this is because the collisions can only occur during the small fraction of the orbit when Hilda objects are close to one of the Trojan clouds. The $\langle P_{\rm i} \rangle$ of HT collisions is not affected by the incomplete Trojan population, due to the normalisation ($n_{\rm p}$) of $P_{\rm i}$. The $\langle P_{\rm i} \rangle$ found for HC collisions is relatively high, reflecting that objects from the two populations can collide during large fractions of their orbits.

The obtained $\langle P_{\rm i} \rangle$ for MM collisions are higher than the main-belt value $\langle P_{\rm i} \rangle$ = 2.86 $\times 10^{-18}\,\rm km^{-2}\,yr^{-1}$ obtained by Bottke et al. (1994). The difference is probably due to the different 'main-belt' used by Bottke and co-workers, they also included Cybele asteroids in their main-belt. Therefore a more reasonable comparison can be made with the result for the main-belt group, which also includes collisions from objects in the Cybele and Hilda populations, but excludes CC collisions. The obtained $\langle P_{\rm i} \rangle$ for the HT and TT populations are also consistent with the mean values obtained by Marzari et al. (1996).

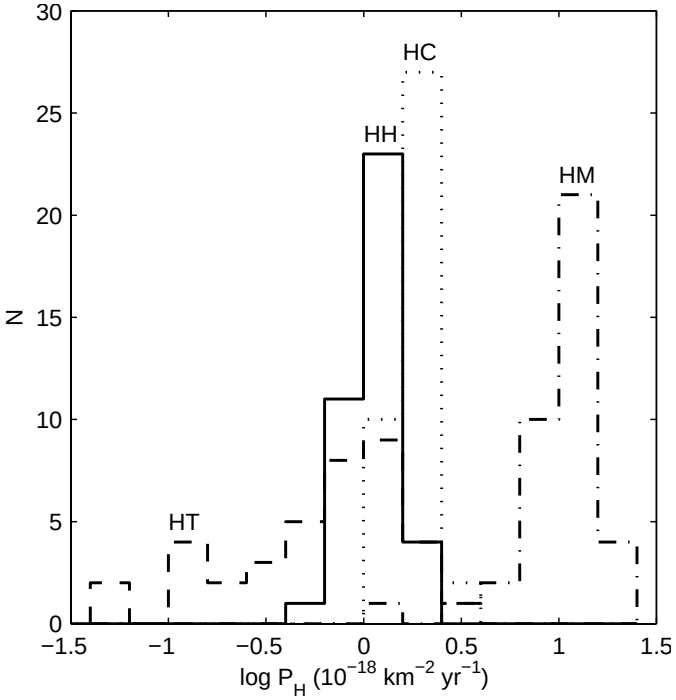

Fig. 4. Histograms of collision probabilities $P_{\rm H}$ for the 39 Hilda asteroids versus different populations: **HH)** Hilda–Hilda, **HM)** Hilda–main-belt, **HC)** Hilda–Cybele, and **HT)** Hilda–Trojan collisions.

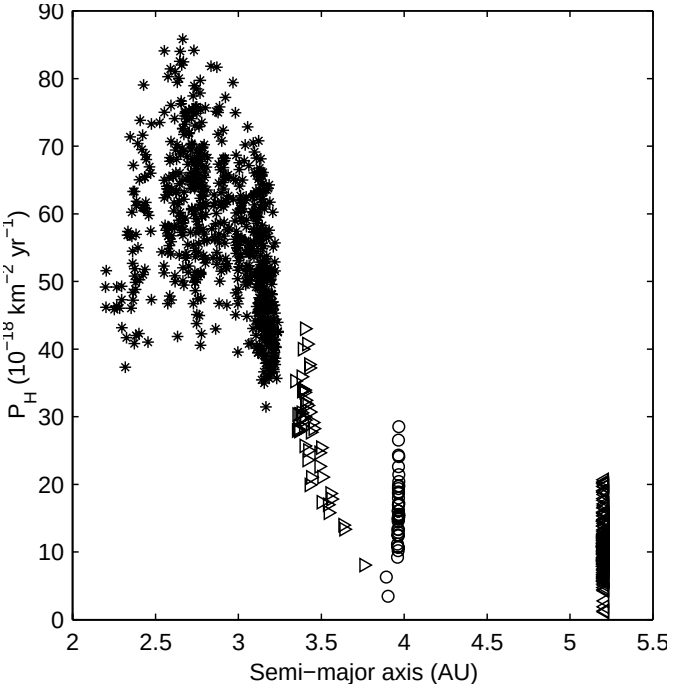

Fig. 5. Collision probability $P_{\rm H}$ versus average semi-major axis during time T for main-belt ($\star$), Cybele ($\triangleright$), Hilda ($\circ$), and Trojan ($\triangleleft$) asteroids. Note that $P_{\rm H}$ for the Trojan asteroids are lower limits due to undiscovered objects with $D \geq 50$ km.

4.2. Collision probabilities of Hilda asteroids

Due to the normalisation of the intrinsic collision probabilities, the relative importance of the entries in Table 4 are not obvious, since $\langle P_{\rm i} \rangle$ is the collision probability per object in the different populations. In order to obtain a better view of the importance of the collisional populations involving Hilda objects, the following collision probability was derived

$$P_{\rm H} = \frac{N}{n_{\rm H} T R^2} \tag{2}$$

where $n_{\rm H}$ is the number of Hilda objects. However, this normalisation is dependent on the numbers of objects in the main-belt, Cybele, Hilda and Trojan groups. When extrapolating the results down to smaller sizes ($D < 50$ km), $P_{\rm H}$ will change if the relative numbers of objects in the groups are different down to the considered size. This dependence of $P_{\rm H}$ is also discussed below in connection to the incomplete Trojan sample. The distributions of $P_{\rm H}$ for the 39 Hilda objects with their interacting populations (HH, HM, HC, and HT) are given in Fig. 4, and mean values are listed in Table 5. The dominating contribution from HM collisions is evident, while the contributions from the HH, HC, and HT populations are quite equal, and about a factor ten smaller then the HM collisions. The $P_{\rm H}$ distributions of HH and HM are quite narrow, indicating similar collision probabilities between most Hilda and Cybele objects, whereas HT collisions have a wide range of collision probabilities. However, the very low $P_{\rm H}$ of HT collisions found for some of the Hilda asteroids are based on few encounters and should be interpreted with some caution.

The collision probabilities $P_{\rm H}$ of the 909 asteroids included in the asteroid sample versus their semi-major axis are given in Fig. 5. The main-belt objects ($\star$) have $P_{\rm H}$ approximately between 40–85 $\times 10^{-18}\,{\rm km}^{-2}\,{\rm yr}^{-1}$ with peak values at about 2.6 AU, and decreasing towards the inner and outer parts of the main-belt. The Cybele asteroids ($\triangleright$) have decreasing $P_{\rm H}$ through the group, ranging from about 45 at 3.3 AU down to $10 \times 10^{-18}\,{\rm km}^{-2}\,{\rm yr}^{-1}$ at 3.6 AU. The Hilda asteroids ($\circ$) at 4.0 AU have $P_{\rm H}$ from about 3 to 30 $\times 10^{-18}\,{\rm km}^{-2}\,{\rm yr}^{-1}$. At 5.2 AU the Trojan asteroids have $P_{\rm H}$ from 2 to 20 $\times 10^{-18}\,{\rm km}^{-2}\,{\rm yr}^{-1}$. The mean values and standard error of $P_{\rm H}$ for the main-belt, Cybele, Hilda, and Trojan groups are listed in Table 5. There is considerable scatter around $\langle P_{\rm H} \rangle$ for individual objects in the populations, therefore $\langle P_{\rm H} \rangle$ of the population is a bad approximation for most individual objects.

The mean collision probability $\langle P_{\rm H} \rangle$ for Hilda asteroids is about 3.5 times lower than for objects in the main-belt, and about 2 times lower than in the Cybele population. The determined $\langle P_{\rm H} \rangle$ of the Trojan asteroids are somewhat lower than for the Hilda asteroids, however, $P_{\rm H}$ of the Trojan asteroids are lower limits due to undiscovered Trojan asteroids with $D \geq 50$ km. Increasing the population of Trojan asteroids larger than 50 km with $\sim 15\%$ will make $\langle P_{\rm H} \rangle$ for the Trojan and Hilda populations about equal. But as noted above the Trojan population may be incomplete by as much as a factor of two. This will increase the collision probabilities among the Trojans up to about a factor of six. This makes is very likely that the Hilda asteroids have the lowest collision probabilities of the asteroids considered in this paper. The main reason for the low $\langle P_{\rm H} \rangle$ of the Hilda as-

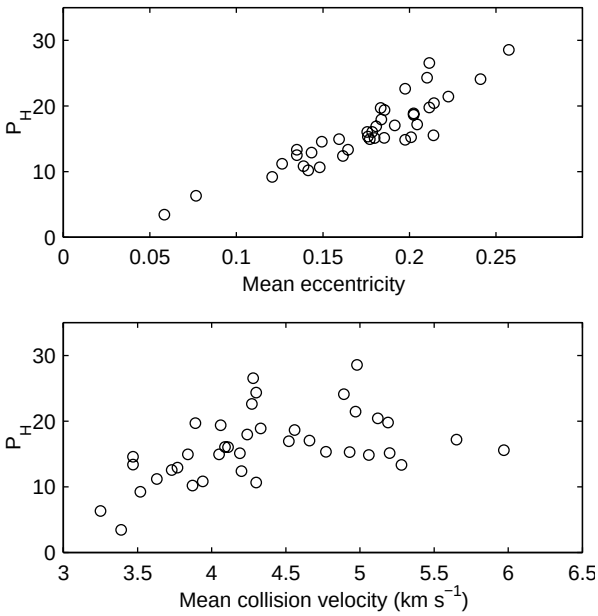

Fig. 6. Collision probability $P_{\rm H}$ (in units of $10^{-18}\,{\rm km}^{-2}\,{\rm yr}^{-1}$) versus mean eccentricity (upper panel), and versus mean collision velocity (lower panel) for 39 Hilda asteroids.

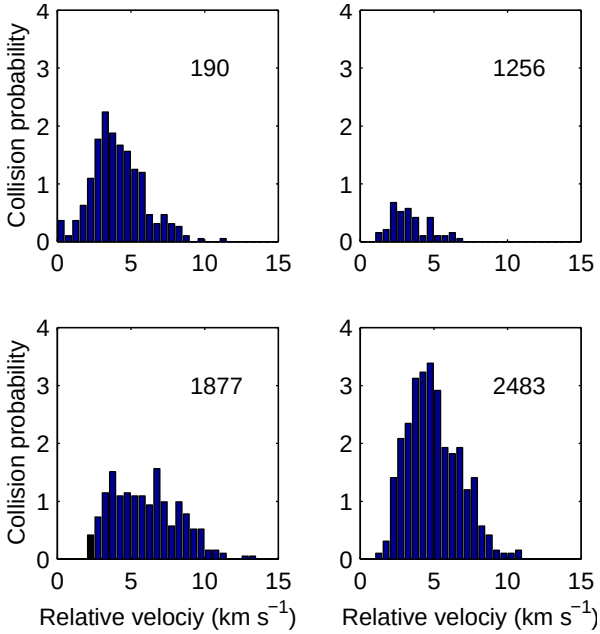

Fig. 7. Collision velocity distributions for four Hilda asteroids: 190 Ismene, 1256 Normannia, 1877 Marsden and 2483 Guinevere. The areas under the histograms are proportional to the collision probability $P_{\rm H}$ (and $P_{\rm i}$) of the objects. The figures are shown to the same scale to facilitate comparison between the objects. The bin size is $0.5\,{\rm km\,s^{-1}}$.

teroids are that they are in 'void regions' during a large part of their orbit, out of reach for both main-belt and Trojan asteroids. Most objects in the main-belt and Trojan clouds can however, collide with objects anywhere in their orbits.

5. Collisional properties of individual Hilda asteroids

The collision probability of the Hilda asteroids are dominated by HM collisions that only occurs when they are relatively close to their perihelia. Depending on the individual eccentricities of the Hilda asteroids they will reach unequally deep into the main-belt. The deeper into the main-belt the Hilda asteroids can reach they will increase their probability of encountering a main-belt asteroid for two reasons. The Hilda orbit will cross the orbits of a larger fraction of main-belt objects, and the Hilda asteroid will be in the 'main-belt space' during a larger fraction of its orbit.

Schubart (1982) showed that the eccentricity of individual Hilda objects oscillates around a fixed mean value for at least 10^5 years. An extension of Schubart's study has been made (unpublished) with a numerical integration taking into account perturbations from Venus to Neptune. The results showed that the Hilda orbits are stable for at least 2×10^6 years. Also Franklin et al. (1993) concluded that the orbits of Hilda asteroids seem to be stable during the history of the Solar System.

The stability of the mean eccentricity gives the expectation that there will be a strong correlation between mean eccentricity and collision probability for Hilda objects. This is also indicated by the wide range of $P_{\rm H}$ among the Hilda asteroids seen in Fig. 5.

This is verified in Fig. 6, which shows a very strong correlation between the mean eccentricity during time T and the collision probability (correlation coefficient r = 0.90). The scatter in the eccentricity-$P_{\rm H}$ correlation is due to objects with higher or lower inclinations than average. Somewhat surprisingly the range in $P_{\rm H}$ among the Hilda asteroids is almost a factor of six when including the two low eccentricity objects (334 Chicago and 1256 Normannia), but the range reduces to a factor of three when excluding these two objects. Note that the eccentricity-$P_{\rm H}$ correlation is not due to the increased orbital velocity close to perihelia of objects with higher eccentricity.

Fig. 6 (lower panel) gives the mean relative velocity versus $P_{\rm H}$ for the Hilda asteroids. The mean velocities range from 3.3 to $6.0\,{\rm km\,s^{-1}}$, and a tentative correlation between $P_{\rm H}$ and $\langle V\rangle$ is indicated in the data (r = 0.46), because larger eccentricities result in both higher collision velocities and higher collision probabilities. The $P_{\rm H}$ plotted in Fig. 6, together with the obtained mean, median, rms, collision velocities and the standard deviations of the velocity distributions are given in Table 6.

To illustrate the scatter of collision properties of the Hilda population, the distribution of collision velocities of four Hilda asteroids are given in Fig. 7. The areas under the histograms are proportional to the collision probability $P_{\rm H}$ (and $P_{\rm i}$) of the objects. In the velocity distribution of 190 Ismene, 3% of the encounters have a very low velocity, $V\sim0.3\,{\rm km\,s^{-1}}$. All these encounters are with the Hilda asteroid 2246 Bowell. This shows that due to the similar shapes of Hilda orbits the relative velocity between two objects can be very low at an encounter, or at a series of encounters. This gives a low velocity tail in the velocity distributions for some of the Hilda asteroids, which is also seen in the velocity distribution of HH collisions in Fig. 1.

Table 6. Collision probabilities $P_{\rm H}$ for the 39 Hilda asteroids obtained with 909 asteroids with $D \geq 50$ km, together with mean, median, and rms collision velocities of the Hilda objects. Also the standard deviations of the collision velocities are given. The intrinsic collision probabilities for the Hilda objects can be calculated with $P_{\rm i} = 39/909 \times P_{\rm H}$.

Hilda asteroid	$P_{\rm H}$ ($10^{-18}\,{\rm km^{-2}\,yr^{-1}}$)	$\langle V \rangle$ ($\rm km\,s^{-1}$)	$V_{\rm median}$ ($\rm km\,s^{-1}$)	$V_{\rm rms}$ ($\rm km\,s^{-1}$)	σ ($\rm km\,s^{-1}$)
153 Hilda	17.0 ± 0.7	4.52	4.21	4.86	1.79
190 Ismene	16.1 ± 0.7	4.11	3.95	4.48	1.80
334 Chicago	6.3 ± 0.5	3.25	2.93	3.53	1.38
361 Bononia	20.5 ± 0.7	5.12	4.91	5.47	1.93
499 Venusia	24.5 ± 0.7	4.30	4.22	4.61	1.65
748 Simeisa	14.9 ± 0.7	4.05	4.02	4.37	1.63
958 Asplinda	15.2 ± 0.7	4.19	4.00	4.50	1.66
1162 Larissa	14.7 ± 0.7	3.47	3.25	3.79	1.53
1180 Rita	16.1 ± 0.7	4.09	4.08	4.41	1.64
1202 Marina	12.6 ± 0.5	3.73	3.58	4.08	1.65
1212 Francette	15.6 ± 0.7	5.97	5.79	6.38	2.25
1256 Normannia	3.5 ± 0.2	3.39	3.16	3.63	1.30
1268 Libya	13.1 ± 0.5	3.77	3.58	4.04	1.47
1269 Rollandia	13.5 ± 0.7	3.47	3.17	3.76	1.45
1345 Potomac	19.8 ± 0.7	5.19	5.01	5.56	2.00
1439 Vogtia	17.9 ± 0.7	4.24	4.12	4.52	1.56
1512 Oulu	18.6 ± 0.7	4.56	4.50	4.87	1.69
1529 Oterma	12.4 ± 0.5	4.20	4.02	4.55	1.75
1578 Kirkwood	26.6 ± 0.9	4.28	4.25	4.58	1.63
1746 Brouwer	10.7 ± 0.5	4.30	3.97	4.65	1.77
1748 Mauderli	19.3 ± 0.7	4.06	3.75	4.40	1.71
1754 Cunningham	15.4 ± 0.7	4.93	4.77	5.28	1.87
1877 Marsden	15.6 ± 0.7	5.97	5.79	6.38	2.25
1902 Shaposnikov	14.9 ± 0.7	5.06	4.96	5.34	1.70
1911 Schubart	22.6 ± 0.7	4.27	4.19	4.56	1.62
2067 Aksnes	19.8 ± 0.7	3.89	3.62	4.22	1.62
2246 Bowell	15.4 ± 0.7	4.77	4.54	5.15	1.94
2312 Duboshin	9.3 ± 0.5	3.52	3.16	3.86	1.59
2483 Guinevere	28.7 ± 0.9	4.98	4.79	5.29	1.79
2760 Kacha	15.2 ± 0.7	5.20	5.02	5.59	2.06
3134 Kostinsky	17.0 ± 0.7	4.66	4.39	4.99	1.79
3577 Putilin	18.8 ± 0.7	4.33	4.09	4.58	1.51
3694 Sharon	10.3 ± 0.5	3.87	3.66	4.16	1.52
3843 OISCA	11.2 ± 0.5	3.63	3.39	3.97	1.62
3990 Heimdal	15.4 ± 0.7	4.77	4.54	5.15	1.94
4317 Garibaldi	21.4 ± 0.7	4.97	4.88	5.27	1.76
5603 Rausudake	11.0 ± 0.5	3.94	3.71	4.24	1.56
5661 Hildebrand	17.2 ± 0.7	5.65	5.54	6.05	2.16
1994 VC_7	13.3 ± 0.7	5.28	5.05	5.55	1.73

The great difference in collisional probability among the Hilda asteroids are illustrated by 1256 Normannia and 2483 Guinevere, which has the lowest and highest $P_{\rm H}$, respectively. The spread in collision velocities among the Hilda population are illustrated by 1256 Normannia ($\langle V \rangle$ = 3.39 $\rm km\,s^{-1}$) and the high inclination object 1877 Marsden (i=17°), which have the highest mean collision velocity ($\langle V \rangle$ = 6.0 $\rm km\,s^{-1}$), and a high velocity tail reaching velocities of about 14 $\rm km\,s^{-1}$.

6. Conclusions

The collision probabilities and collision velocities of the asteroid belt have been derived and analysed with emphasis on the Hilda asteroids. Good agreement is found (where comparisons are possible) between results obtained in this study and the results of earlier studies of main-belt and Trojan asteroids by Bottke et al. (1994) and Marzari et al. (1996). The analysis of the collision properties of Hilda asteroids have given the following new results:

i) Out of ten collisions experienced by a Hilda asteroid, approximately seven of these are with main-belt objects, and the remaining three collisions are about equally distributed between objects in the Cybele, Hilda, and Trojan groups.

ii) The mean collision probabilities are lower for Hilda asteroids than for any other group of asteroids (i.e., the main-belt, Cybele and Trojan groups), indicating that the Hilda asteroids are less collisionally evolved than other groups of asteroids. Since not all Trojan asteroids with $D \geq 50$ km are discovered at this time, the frequency of collisions between Hilda and Trojan asteroids is underestimated. However, this will not alter the conclusion above because of the small relative importance of HT collisions.

iii) The range of collision probabilities for individual objects in the Hilda group is about a factor of six. This is larger than the range found in the main-belt and Cybele groups, and is comparable to the spread in collision probabilities among the Trojan asteroids.

iv) There is a strong correlation of collision probability with eccentricity for Hilda asteroids, giving rise to the large range in collision probabilities among Hilda objects. This is due to the possibility of Hilda objects to encounter a larger fraction of the objects in the main-belt when the eccentricities of their orbits are larger. There is also a preference for Hilda asteroids with high collision probability to have higher mean collision velocities. This is due to that larger eccentricities results in both higher velocities and higher collision probabilities.

v) Two of the Hilda objects, 334 Chicago and 1256 Normannia, have very low collision probabilities and collision velocities, indicating that they may be among the least collisionally evolved objects of the 909 asteroids in the sample.

vi) The mean collision velocity of Hilda asteroids is $4.6\,\mathrm{km\,s^{-1}}$, which is about $0.5\,\mathrm{km\,s^{-1}}$ lower than the mean velocity in the main-belt. The mean velocity for collisions among Hilda asteroids is only $3.1\,\mathrm{km\,s^{-1}}$, (confirming the result by Marzari et al. 1996). However, these collisions contribute less than 10% to the collision probabilities of Hilda objects. A low velocity tail (down to $V \approx 0.3\,\mathrm{km\,s^{-1}}$) from mutual Hilda collisions is found, indicating the occurrence of very 'soft' collisions between Hilda asteroids.

vii) The non-isotropic collision geometries among asteroids found in earlier investigations, with large velocity components perpendicular to the ecliptic plane, are confirmed. However, the collision geometries for Hilda objects are more isotropic than for the other groups of asteroids, due to a small inclinations of the Hilda type orbits.

Acknowledgements. P. Magnusson, C.-I. Lagerkvist, and A. Erikson are thanked for their valuable comments on the manuscript.

References

Bottke W. F., Nolan M. C., Greenberg R., Kolvoord R. A., 1994, Icarus 107, 255

Bowell E., 1997, The asteroid orbital elements database, WWW-page, ftp://ftp.lowell.edu/pub/elgb/astorb.html.

Bowell E., Hapke B., Domingue D., Lumme K., Peltoniemi J., Harris A. W., 1989, Application of photometric models to asteroids. In: Binzel R.P., Gehrels T., Matthews, M.S. (eds.) Asteroids II, Univ. of Arizona Press, Tuscon. p. 524.

Cellino A., Zappalà, V., Farinella P., 1991, MNRAS 263, 561.

Dahlgren M., Lagerkvist C.–I., 1995, A & A 302, 907.

Dahlgren M., Lagerkvist C.–I., Fitzsimmons A., Williams I. P., Gordon M., 1997, A & A 323, 606.

Everhart E., 1985, An efficient integrator that uses Gauss–Radau spacings. In: A. Carusi G B. Valsecchi (eds.) Dynamics of Comets: Their Origin and evolution, Proceedings of the IAU Coll. 83, Reidel, Dordrecht p. 185.

Farinella P., Davis D. R., 1992, Icarus 97, 111

Franklin F., Lecar M., Murison M., 1993, Astron. J. 105, 2336

Lagerkvist C.–I., Hernius O., Lindgren M., Tancredi G., 1996, The Uppsala-ESO Survey of Asteroids and Comets–UESAC, In: A. Lopez Garcia et al. (eds.) The third International Workshop on Positional Astronomy and Celestial Mechanics. p. 9.

Marzari F., Scholl H., Farinella P., 1996, Icarus 119, 192

Schubart J., 1982, A & A 114, 200.

Tedesco E.F, Veeder G.J., 1992, IMPS albedo and diameters catalog. In: Tedesco, E.F., (eds.) Infrared Astronomical Satellite Minor Planet Survey. Phillips Laboratory Technical Report No. PL-TR-92-2049. Hanscom Air Force Base, MA. p. 243

Vedder J. D., 1996, Icarus 123, 436.

Wetherill G. W., 1967, J. Geophys. Res. 72, 2429

Öpik E. J., 1951, Proc. R. Irish Acad. A54, 165.